Biotechnology and Bioengineering

WILEY

BIOTECHNOLOGY AND BIOENGINEERING

ARTICLE

Highly Efficient Enzymatic Catalytic Transformation for the Synthesis of Rare Ginsenoside Compound K (CK) and Its Bioactivity Study

Hao Tang[1] | Shihua Han[2] | Zidan Li[1] | Yiwen Jiang[3,4] | Meimei Fu[4] | Zhuoyi Huang[4] | Lei Jia[3] | Fengrui Song[1,4] | Jianguo Huang[1] | Gloria B. Kim[5] | Jinshan Guo[3] | Zhihui Lu[1,4]

[1]Suzhou Zhentai Biotechnology Co., Ltd, Kunshan Industrial Technology Research Institute, Suzhou, P. R. China | [2]Dongguan Qingxi Hospital, Dongguan City, P. R. China | [3]Department of Biomaterials and Stem Cells, Suzhou Institute of Biomedical Engineering and Technology, Chinese Academy of Science, Suzhou, P. R. China | [4]Regenerative Medicine and Tissue Repair Research Center, Huangpu Institute of Materials, Guangzhou, P. R. China | [5]Department of Physiology and Biomedical Engineering, Department of Immunology, Mayo Clinic Arizona, Scottsdale, Arizona, USA

Correspondence: Gloria B. Kim (Kim.Gloria2@mayo.edu) | Jinshan Guo (guojinshan@sibet.ac.cn; jsguo4127@163.com) | Zhihui Lu (luzhihui107@sohu.com)

Received: 4 March 2026 | **Revised:** 8 June 2026 | **Accepted:** 13 June 2026

Keywords: anti-aging | bioconversion | compound CK | ginsenoside Rb1 | recombinant β-glycosidase

ABSTRACT

As a principal metabolite of ginsenosides, compound K (CK) exhibits remarkable antioxidant, anti-inflammatory, antidiabetic, and anticancer bioactivities. However, CK is naturally scarce in ginseng and its industrial application is limited by the lack of efficient deglycosylating enzymes for large-scale CK bioproduction. Here, we report a synthetic biology-driven approach for high-yield CK production *via* recombinant β-glycosidase-mediated bioconversion of the polar ginsenoside Rb1. The β-glycosidase-encoding gene was introduced into *Escherichia coli* BL21 (DE3), and the resulting engineered strain produced 2.1 g/L β-glycosidase in shake flasks and 10.1 g/L in a 5-L fermentor. The crude β-glycosidase exhibited excellent enzymatic activity; at a concentration of 1.5 g/L, it converted 95% of the Rb1 substrate (initial concentration 10 g/L) to CK within 4 h. *In vitro* studies demonstrated CK's high cytocompatibility and potent anti-aging effects, including suppression of reactive oxygen species (*via* upregulation of superoxide dismutase, catalase, and glutathione peroxidase), enhanced collagen I, III and elastin synthesis, and matrix metalloproteinase-1 inhibition. These findings highlight CK as a promising candidate for anti-wrinkle formulations, supported by the feasibility of scalable bioproduction.

1 | Introduction

Ginseng (*Panax ginseng* C. A. Meyer), a perennial herbaceous plant of the genus *Panax* in the family *Araliaceae*, holds a uniquely esteemed and irreplaceable position in Chinese materia medica, and is traditionally recognized as the "King of Herbs" (Dong et al. 2022; Yun 2001). Its dual medicinal and dietary applications span millennia, and in 2012, China's former Ministry of Health officially approved cultivated ginseng (≤ 5-year growth period) as a novel food resource. The pharmacological effects of ginseng are primarily attributed to its ginsenosides, which are broadly classified into predominant and rare subtypes based on their relative abundance. Predominant ginsenosides accounts for approximately 80% of the total ginsenoside content, whereas rare ginsenosides are thermodynamically transformed derivatives (Koh et al. 2015; Mancuso and Santangelo 2017; Son et al. 2008). Notably, rare ginsenosides can be bio-converted from predominant ginsenosides through microbial metabolism in the intestinal tract (Kim et al. 2013). Despite their low natural abundance, rare ginsenosides

Hao Tang, Shihua Han and Zidan Li contributed equally to this work.

exhibit enhanced bioavailability and superior cellular membrane permeability due to their smaller molecular dimensions, contributing to their distinct biological activities (Fu 2019).

Ginsenoside compound K (CK) is a representative rare ginsenoside that is absent in fresh ginseng. It has been extensively studied for its anti-inflammatory (Chen et al. 2019; Lee et al. 2019), antidiabetic (Yoon et al. 2007) and anticancer (Chae et al. 2009; Li et al. 2019; Yin et al. 2021) properties. Pharmacokinetic studies have shown that orally administered ginsenoside Rb1 is metabolically converted to CK for systemic absorption. However, this bioconversion is limited by multiple physiological factors in humans, resulting in low systemic exposure to CK through this metabolic pathway (Shin et al. 2005). Current CK production strategies can be primarily divided into chemical transformation and biotransformation. Among these approaches, enzymatic biotransformation offers distinct advantages over chemical methods, including shorter reaction times, milder reaction conditions, higher conversion efficiency, greater substrate specificity, and improved environmental sustainability. Nevertheless, although reported β-glucosidases can specifically convert ginsenoside Rb1 to CK, their catalytic efficiency remains insufficient for industrial-scale manufacturing (Noh et al. 2009; Park et al. 2001; Qin et al. 2008). This underscores the critical importance of enzyme selection and optimization in the bioconversion process.

In this study, we developed a high-yield microbial cell factory for β-glycosidase-production by heterologously expressing a codon-optimized β-glycosidase-encoding gene in the *E. coli* BL21 (DE3) chassis. The engineered strain achieved a β-glycosidase production levels of 2.1 g/L in shake flasks and 10.1 g/L in a 5-L fermentor. Additionally, the recombinant β-glycosidase exhibited excellent activity, converting 95% of ginsenosides to CK within 4 h. The purified CK production was further evaluated in *in vitro* cytocompatibility and bioactivity studies, which demonstrated CK′s favorable cytocompatibility and potent anti-aging effects achieved through suppression of reactive oxygen species (ROS), stimulation of collagen I, III, and elastin synthesis, and inhibition of matrix metalloproteinase-1 (MMP-1).

2 | Materials and Methods

2.1 | Plasmids, Bacterial Strains, Cell Lines, and Reagents

Escherichia coli DH5α was used as the cloning host, and *E. coli* BL21 (DE3) was selected as the chassis for recombinant β-glycosidase overexpression. The pET28a(+) plasmid was used as the expression vector for His-tagged β-glycosidase overexpression. Kanamycin was purchased from Sangon Biotech (Shanghai, China). Polymerase chain reaction (PCR) was performed using Phanta Max Super-Fidelity DNA polymerase (Vazyme Biotech, Nanjing, China) with primers synthesized by RuiBiotech (Beijing, China). Restriction endonucleases were purchased from Thermo Fisher Scientific (Waltham, MA, USA). PCR products or endonuclease digestion products were purified using a gel extraction kit (Tiangen Biotech, Beijing, China). The recombinant plasmid was constructed by Gibson assembly using the Hieff Clone One Step Cloning Kit (Yeasen, Shanghai, China). DNA sequencing was performed by RuiBiotech (Beijing, China). Plasmid DNA was isolated from *E. coli* using the TIANpure Mini Plasmid Kit (Tiangen Biotech, Beijing, China). 40% Rb1 substrate was purchased from Herbest (Baoji, China) and CK standard was from Macklin (Shanghai, China).

Human immortalized keratinocyte (HaCaT) and skin fibroblast (HSF) cell lines were purchased from the Cell Bank of the Chinese Academy of Sciences (Shanghai, China), with provider-certified authentication. All cell lines showed normal size, karyotype, morphology, and no contamination were observed. All cell culture-related reagents were purchased from Gibco (Grand Island, NY, USA). CCK-8 kit was from Beyotime Biotechnology (Shanghai, China). Superoxide dismutase (SOD), catalase (CAT), and glutathione peroxidase (GSH-Px) activity assays were performed using commercial kits (Jiancheng, Nanjing, China).

2.2 | Construction of the Recombinant Plasmid and Strain

The codon-optimized β-glycosidase gene *bglA** was synthesized *de novo* (RuiBiotech, Beijing, China). The *bglA** gene was PCR-amplified and cloned into EcorI/NotI-digested pET28a(+) vector. The resulting plasmid, pET-*bglA**, was transformed into *E. coli* BL21 (DE3), and the confirmed recombinant strain was designated as BL21/*bglA**. The plasmid construct was verified by colony PCR and Sanger sequencing.

2.3 | Culture Medium and Cultivation Conditions

For the screening of *E. coli*, cells were maintained on Luria-Bertani (LB) agar plates or grown in LB liquid medium containing 50 μg/mL kanamycin at 37°C with shaking at 220 rpm. For β-glycosidase production, the seed culture was incubated at 37°C for 12–16 h with shaking at 220 rpm. For shake-flask fermentation, 1 mL of seed culture was inoculated into a 250-mL flask containing 50 mL of LB medium and incubated at 37°C with shaking at 220 rpm until the OD_{600} reached approximately 0.5. Protein expression was then induced by adding isopropyl β-D-1-thiogalactopyranoside (IPTG) to a final concentration of 0.5 mM, followed by incubation at 20°C for 19 h. Fed-batch fermentation was performed in a 5-L fermentor (Baoxing, Shanghai) containing 2 L of fermentation medium, which consisted of (per liter): 10 g of glycerol, 11.5 g of yeast extract, 19.5 g of tryptone, 4 g of $(NH_4)_2SO_4$, 18 g of K_2HPO_4 and 1.2 g of $MgSO_4$. The pH was maintained at 7.0 by automated addition of ammonia solution throughout the fermentation. Dissolved oxygen was kept above 20% by adjusting the stirring speed from 300 to 600 rpm with sterile air supplied at 1 vvm. The fermentation temperature was maintained at 37°C until the OD_{600} reached about 20, after which protein expression was induced with 0.5 mM IPTG, and cultivation continued for an additional 16 h at 25°C. The feeding medium consisted of (per liter): 400 g of glycerol, 55 g of yeast extract, and 20 g of tryptone. Fermentation samples were collected at designated time points for analysis.

2.4 | Analysis of Strain Growth as Well as Quantitation of β-Glycosidase and Glycerol Level

To analyze strain growth, OD_{600} was determined using a microplate reader (Tecan Reader). Supernatant proteins from the cell lysates of BL21/*bglA** were assessed by sodium dodecyl sulfate polyacrylamide gel electrophoresis (SDS-PAGE), and β-glycosidase levels were then quantified using the Enhanced BCA Protein Assay Kit (Beyotime Biotechnology, Shanghai, China) in combination with band density analysis using ImageJ software. To characterize glycerol consumption during fermentation, the concentration of residual glycerol was determined using a biosensor analyzer (M-100).

2.5 | | β-Glycosidase Enzymatic Assay

The enzymatic reaction was performed in a 1-L flask containing a 300-mL reaction mixture. The mixture consisted of 1.5 g/L crude β-glycosidase, 10 g/L ginsenoside Rb1, and reaction buffer (20 mM acetic acid-sodium acetate buffer, pH 5.5). After incubation at 85°C for 4 h, the mixture was centrifuged at 10,000 × g for 10 min. The precipitate was collected and dissolved in ethanol. Subsequently, the supernatant was centrifuged again at 10,000 × g for 10 min and then filtered through a 0.22-μm syringe filter. Quantification of Rb1 and CK was performed on an Agilent 1260 HPLC system equipped with a Suprsil C18 column (5 μm, 250 × 4.6 mm) and a diode array detector set at 203 nm. Solvent A (water) and solvent B (acetonitrile) were used with the following gradient: 0–10 min, 30% B; 10–35 min, 30%–55% B; 35–50 min, 55% B; and 50–60 min, 55%–30% B. Chromatographic separation was achieved at a flow rate of 1.0 mL/min with a 5-μL injection volume.

2.6 | Isolation and Purification of Compound CK

The isolation and purification of CK produced *via* the enzymatic transformation was performed as described elsewhere (Li et al. 2009).

2.7 | Cytotoxicity Assays

The cytotoxicity of CK was evaluated using a CCK-8 assay according to the manufacturer's instruction. Briefly, CK was dissolved in complete medium and filtered through a 0.22-μm syringe. HSF cells were seeded into 96-well plates at a density of 4×10^4 cells/mL, and cultured at 37°C for 24 h. Subsequently, the culture medium was replaced with fresh medium containing CK at concentrations of 10, 20, 30, 40 μg/mL, or left untreated as a control, followed by additional 24 h incubation. After treatment, the culture solution was replaced with a CCK-8 solution for 2 h at 37°C. Then the absorbance at 450 nm was detected.

2.8 | Enzyme-Linked Immunosorbent Assay (ELISA) for Collagen I, III, Elastin and MMP-1 Expression

The expression levels of collagen I, III, Elastin and MMP-1 were determined using commercial ELISA kits (Bioswamp, Wuhan, China). HSF cells seeded into 12-well plates (80%–90% confluency) were treated with CK (10–40 μg/mL) as described on isolation and purification of compound CK. Conditioned media were collected after 24 h' incubation and analyzed according to the manufacturer's instructions.

2.9 | Intracellular ROS Detection

HaCaT cells were treated with 50 μM H_2O_2 in 24-well plates (80%–90% confluency) at 37°C for 30 min, followed by treatment with CK (10–40 μg/mL) for 24 h. Intracellular ROS levels were detected using a Reactive Oxygen Species Assay Kit (Jiancheng, Nanjing, China). Fluorescence images were acquired using an inverted fluorescence microscope, and fluorescence intensity was quantified using ImageJ software.

2.10 | | SOD, CAT, and GSH-Px Activity Assays

Following the same pretreatment used for the ROS assay, cell lysates were prepared by ultrasonic disruption. After centrifugation (12,000 × g, 15 min, 4°C), the supernatants were collected, and the activities of SOD, CAT, and GSH-Px content were analyzed as described by the manufacturer's instructions.

2.11 | Statistical Analysis

Except for 5-L batch fermentation, all experiments were performed in triplicate. Data with error bars represent the mean ± standard deviation. Statistical significance was evaluated using an unpaired two-tailed Student's *t*-test by GraphPad Prism 8. Differences were considered significant at $p < 0.05$ (*), $p < 0.01$ (**), and $p < 0.001$ (***), while nd indicates no significant difference.

3 | Results

3.1 | Heterologous Expression of β-Glycosidase in the *E. coli* BL21 (DE3) Chassis

E. coli BL21 (DE3) was selected as the host strain for β-glycosidase overexpression. The *bglA** gene was cloned in the pET28a (+) plasmid and expressed under an IPTG-inducible T7 promoter (Figure 1A). The resulting recombinant strain, BL21/*bglA**, was inoculated and cultivated *via* shake-flask fermentation. SDS-PAGE analysis of intracellular proteins revealed a prominent band at approximately 62.6 kDa in the supernatant following sonication, indicating high soluble expression level of β-glycosidase in BL21/*bglA** (Figure 1B). Under shake-flask conditions, β-glycosidase production reached 2.1 g/L after 21 h (Figure 2A).

3.2 | | *In Vitro* Conversion of CK From Rb1 by β-Glucosidase With High Conversion Efficiency

The crude β-glucosidase obtained from BL21/*bglA** was further applied in the *in vitro* enzymatic production of CK. HPLC analysis revealed the appearance of a new peak at a retention time of 39.9 min, corresponding to the enzymatic reaction

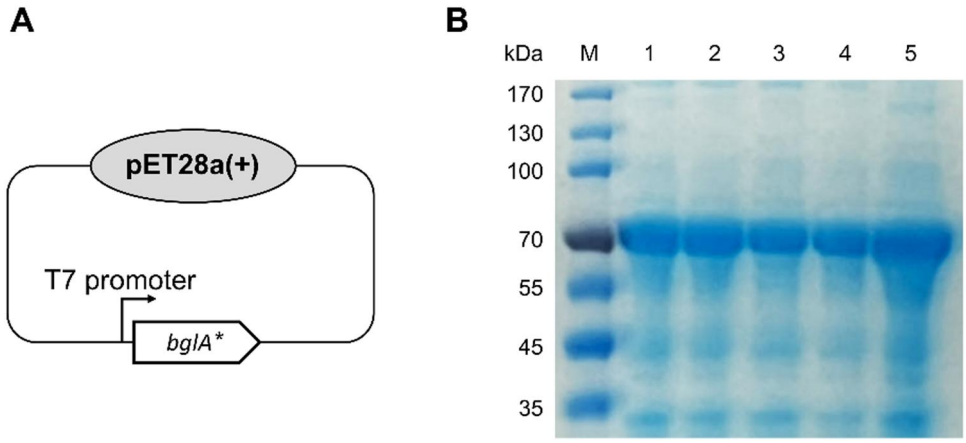

FIGURE 1 | (A) Schematic diagram of the pET-*bglA** plasmid. (B) SDS-PAGE analysis of the supernatant containing purified His-tagged β-glycosidase. M: molecular weight markers; Lanes 1-5: supernatant samples. To further evaluate the performance of the BL21/*bglA** strain, fed-batch fermentation was carried out in a 5 L fermentor. As shown in Figure 2B, the OD_{600} rapidly increased to 1.3 within 8 h after inoculation, with no observable lag phase. β-glycosidase production continued to increase throughout batch fermentation, ultimately reaching 10.1 g/L after 32 h.

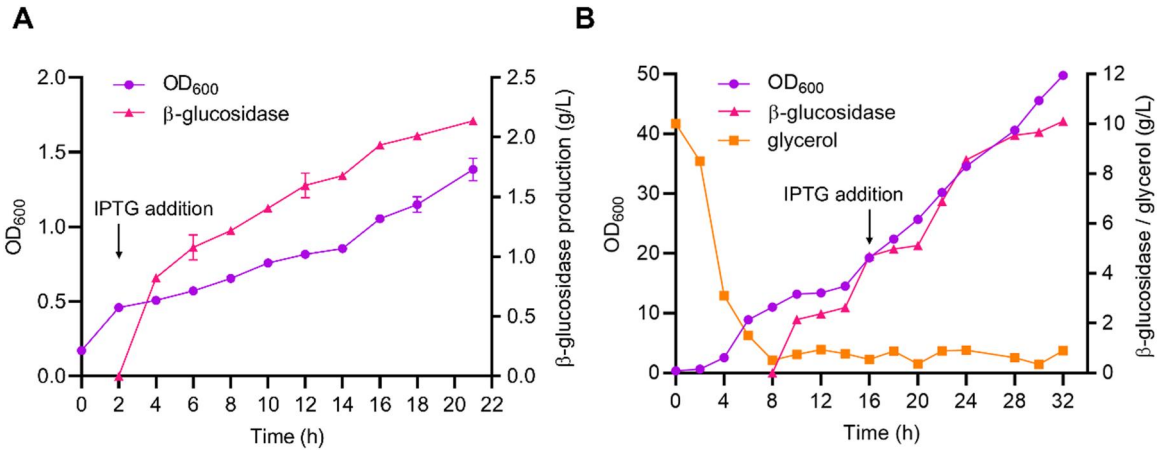

FIGURE 2 | Fermentation profiles of cell growth and β-glucosidase production by BL21/*bglA** strain in shake flasks (A) and a 5-L fermentor (B).

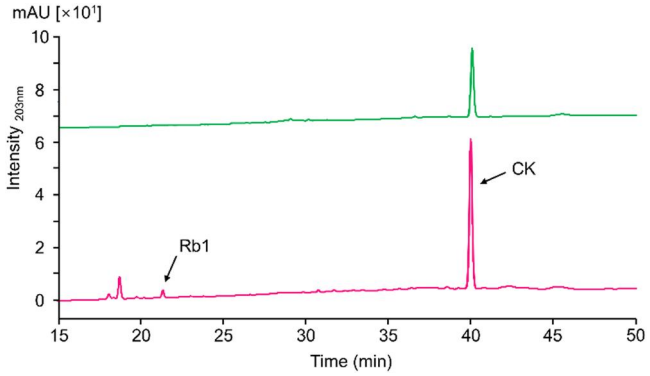

FIGURE 3 | HPLC analysis of components in the enzymatic reaction system after 4 h of catalysis (bottom trace). The CK standard serves as a control (top trace).

product. This peak retention time matched that of the CK standard (Figure 3). In addition, the time-dependent enzymatic assay showed that the product amount increased steadily as the Rb1 substrate was consumed, eventually reaching a plateau (Figure 3). After 4 h, Rb1 was nearly exhausted, and no intermediate products such as Rd were detected (Figure 3). Collectively, these results demonstrate that β-glucosidase effectively catalyzed the bioconversion of ginsenoside Rb1 to CK, achieving a high conversion rate of 95% within 4 h using crude enzyme (Figure 3). Furthermore, CK with a purity of 70% was successfully obtained for subsequent experiments.

3.3 | | CK Derived From Rb1 Exhibited Favorable Cytocompatibility

The *in vitro* cytotoxicity of CK was evaluated using the CCK-8 assay, and its effects on HSF cell proliferation were assessed using both CCK-8 and Live/Dead Staining. As shown in Figure 4A, CCK-8 cells exposed at CK concentrations ranging from 10 to 40 μg/mL maintained viability levels comparable to the untreated control group. This dose-dependent analysis confirms the non-cytotoxic nature of CK within the tested concentration range. As shown in Figure 4B,C, HSF cells exhibited favorable conditions in all tested groups, with an increase in cell numbers and no significant cell death was observed. Cell proliferation slowed down as the concentration of CK increased, suggesting that CK with a certain concentration range can promote cell proliferation.

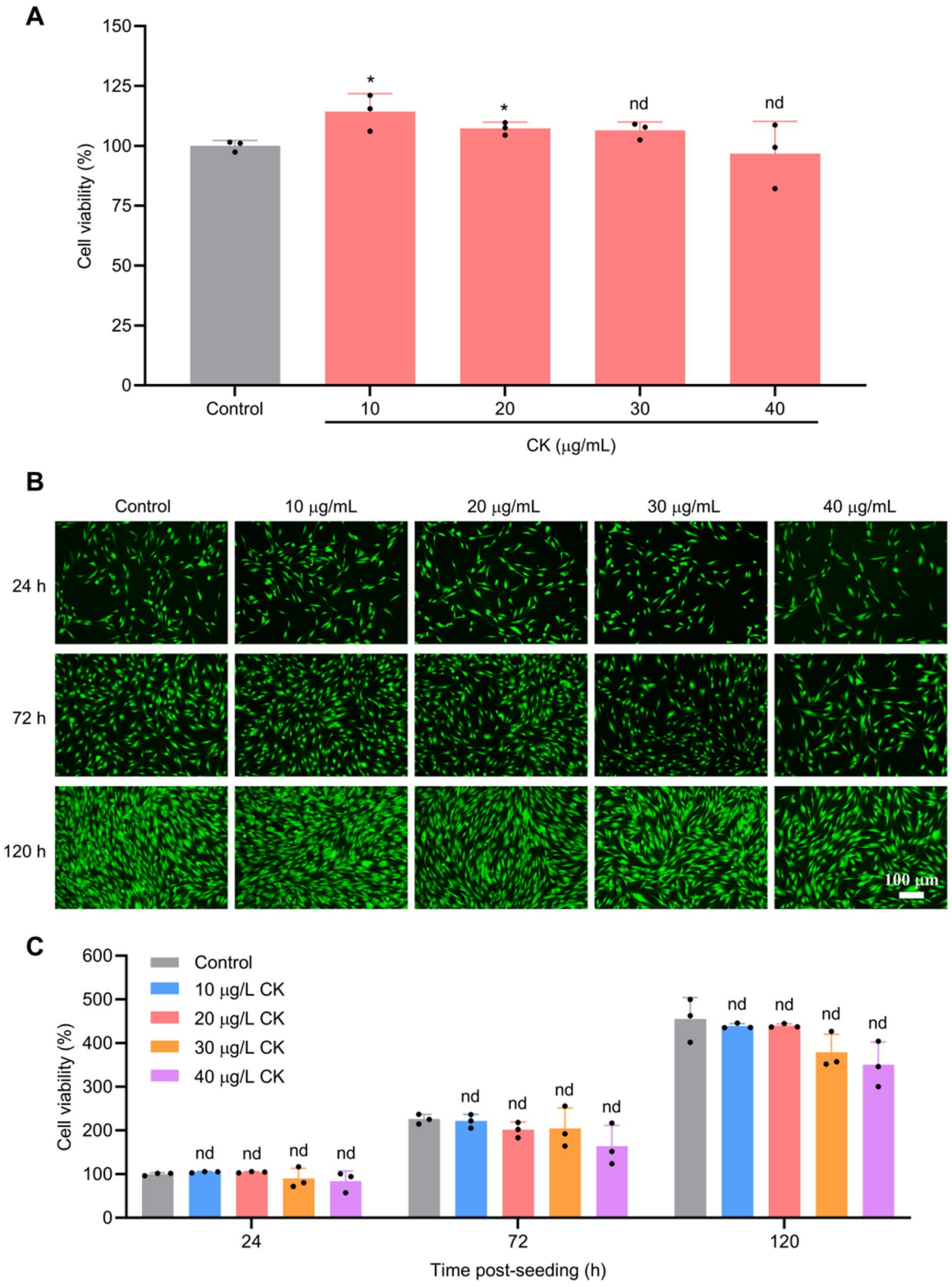

FIGURE 4 | Biocompatibility of CK. (A) Effect of different concentrations (10, 20, 30, and 40 μg/mL) of CK on cell viability by CCK-8 after 24-h treatment. Representative Live/Dead images (green fluorescence indicates live cells stained with Calcein-AM) (B) and quantitative cell amounts (C) of different concentrations (10, 20, 30, and 40 μg/mL) of CK for 24 h, 72 h, and 120 h. Error bars show mean ± SD ($n = 3$).

3.4 | Antioxidant Effects of CK on H_2O_2-Induced Oxidative Stress in HaCaT Cells

As a key contributor to intrinsic skin aging and photoaging, overproduced ROS facilitate wrinkle initiation and skin aging by impairing collagen architecture, cellular viability, skin barrier function and epidermal structure; hence, ROS elimination and neutralization serve as an essential pathway for anti-aging and anti-wrinkle skin care (Papaccio et al. 2022). To evaluate the antioxidant potential of CK, the HaCaT cells pretreated with

H_2O_2 were rescued by CK, and the intracellular ROS levels in the treated HaCaT cells were measured using DCF-DA fluorescence probe. As shown in Figure 5A,B, treatment with CK (10–40 μg/mL) resulted in a dose-dependent reduction in H_2O_2-induced fluorescence intensity, comparable to the effect observed with 0.05% vitamin E, indicating that CK effectively mitigates oxidative stress. Further analysis of antioxidant enzyme activity revealed differential responses. CAT activity showed no significant changes at 10–20 μg/mL CK but increased by 63.3% at 30 μg/mL (Figure 5C). GSH-Px activity exhibited a dose-dependent enhancement, increasing by 72.5%, 102.9%, and 282.6% at 10, 20, and 30 μg/mL CK, respectively (Figure 5D). SOD activity was significantly elevated across all tested CK concentrations (Figure 5E). These findings indicate

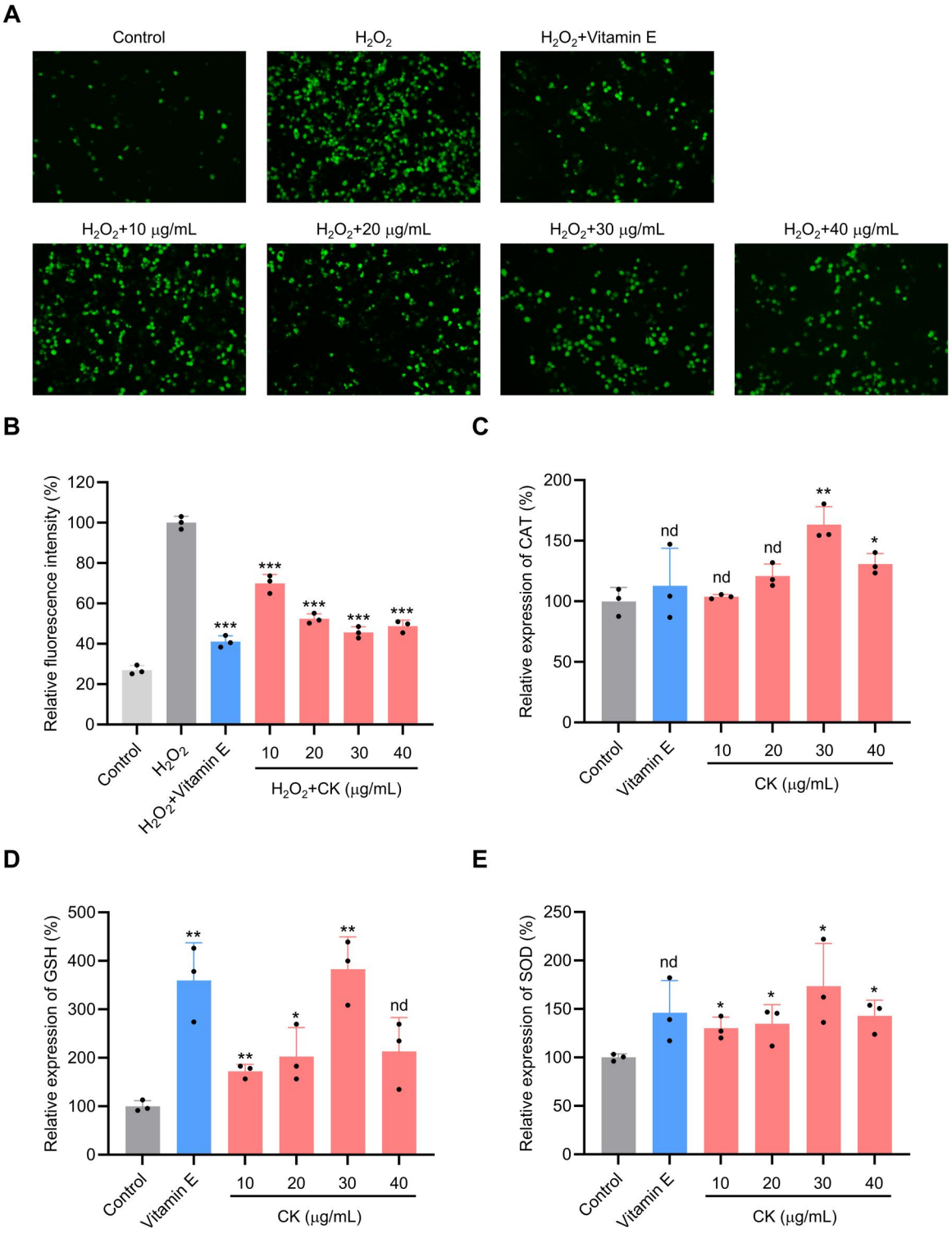

FIGURE 5 | Effects of CK (10, 20, 30, and 40 μg/mL) on ROS levels and antioxidant enzymes in H_2O_2-treated HaCaT cells. (A) ROS level visualized by fluorescence microscopy. (B) Quantification of ROS levels. The effects of different concentrations of CK on the expression of CAT (C), GSH (D) as well as SOD (E). Vitamin E (0.05%) served as a positive control. Error bars show mean ± SD ($n = 3$).

that CK not only directly scavenges free radicals but also enhances intracellular antioxidant defenses by stimulating the activity of key antioxidant enzymes.

3.5 | | CK Promotes the Synthesis of Collagen I, III and Elastin

Collagen I, collagen III, and elastin are key extracellular matrix (ECM) components that play pivotal roles in maintaining skin structure, elasticity, and firmness. A reduction in their synthesis or an increase in their degradation can directly accelerate skin aging (Wang et al. 2025). As shown in Figure 6A, collagen I synthesis was significantly upregulated, increasing by 68.9% and 84.2% at 20 and 30 μg/mL CK comparing with that of the control, respectively, followed by a decline to 77.1% at 40 μg/mL. Collagen III levels were significantly elevated across all CK concentrations from 20 to 40 μg/mL, with increases ranging from 49.3% to 85.0% (Figure 6B). Elastin production peaked at 30 μg/mL CK, showing a 24.8% increase relative to control (Figure 6C).

3.6 | Inhibitory Effect of CK on MMP-1 Secretion

MMP-1 is a matrix-degrading enzyme that contributes significantly to skin aging by breaking down collagen and disrupting ECM integrity. To evaluate the regulatory effect of CK on MMP-1 secretion, we performed ELISA analysis using vitamin E as a positive control. As shown in Figure 6D, CK treatment (10–40 μg/mL, 24 h) elicited a concentration-dependent suppression of MMP-1 expression in HSF cells, achieving 58.9% inhibition at 30 μg/mL. Notably, this inhibitory effect was 1.3-fold higher than that observed with 0.05% vitamin E (44.3% reduction), highlighting CK's potential as a novel MMP-1 modulator.

4 | Discussion

Ginseng has been valued as a prestigious medicinal and edible resource in East Asian countries for millennia (Dong et al. 2022). Notably, natural ginseng extracts contain negligible amounts of the rare ginsenoside CK, distinguishing it from abundant polar ginsenosides such as Rb1 (Koh et al. 2015; Mancuso and Santangelo 2017; Son et al. 2008). Polar ginsenosides can undergo deglycosylation catalyzed by glycosidases to generate CK, which exhibits superior physiological bioactivity (Pan et al. 2018). This biochemical pathway forms the foundation for biocatalytic production of CK from relatively low-cost conventional ginsenoside feedstocks. While extensive research efforts have been devoted to optimizing the conversion of common ginsenosides to CK, substantial room remains for

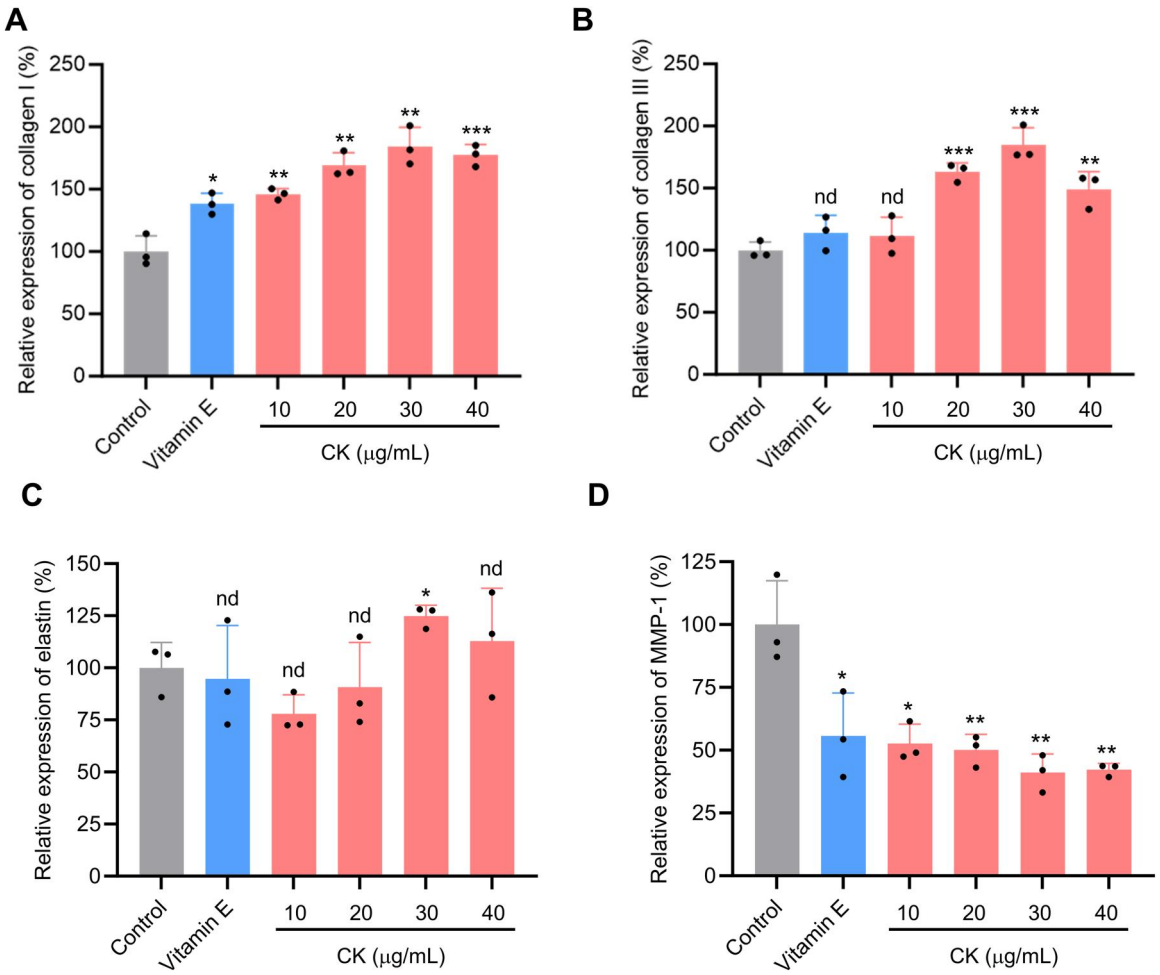

FIGURE 6 | Effects of CK on expression levels of collagen I (A); III (B) elastin (C); and MMP-1 (D) in HSF cells. The vitamin E (0.05%) serves as a control. Error bars show mean ± SD ($n = 3$).

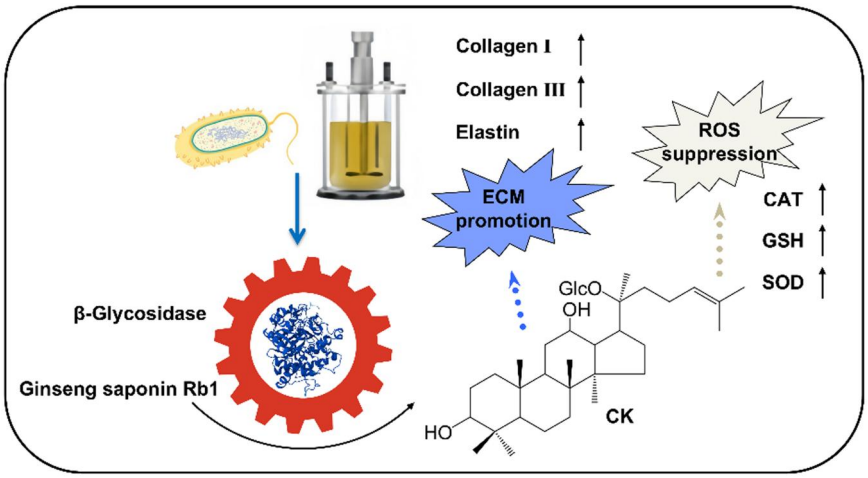

FIGURE 7 | Schematic diagram of β-glucosidase bio-production, β-glucosidase-catalyzed conversion of Rb1 to CK, and the anti-aging activity of CK.

improvement in both glycosidase performance and industrial scalability (Noh et al. 2009; Park et al. 2001; Qin et al. 2008).

In the present study, *E. coli* BL21 (DE3) was selected as the host strain for recombinant glycosidase production due to its short fermentation cycle and well-established high-density fermentation protocols. Through heterologous expression of a codon-optimized β-glycosidase gene, enzyme titers of 2.1 and 10.1 g/L were achieved in shake-flask cultures and 5-L fed-batch fermentations, respectively (Figure 2). Critically, the recombinant enzyme displayed remarkable catalytic efficiency, converting 95% of ginsenoside Rb1 to CK within 4 h using crude enzyme containing broth (Figure 3). This represents a substantial advancement over previous reporting lower conversion rates or requiring costly purified enzymes, which hindered industrial scalability. Collectively, this work demonstrates a synthetic biology-driven strategy for high-yield CK production *via* recombinant β-glycosidase-mediated bioconversion, positioning CK as a promising bioactive ingredient for anti-aging applications (Figure 7). These findings highlight the transformative potential of microbial cell factories in addressing the bottleneck of rare ginsenoside supply for commercial applications.

Furthermore, *in vitro* bioactivity assays comprehensively validated the multifaceted anti-aging mechanisms of CK. CK exerted potent antioxidant effects by suppressing H_2O_2-induced ROS accumulation in HaCaT cells, likely mediated through the upregulation of SOD, CAT, and GSH-Px activities. Intriguingly, CK exhibited concentration-dependent differential regulation of the measured endpoints, with a consistent optimal bioactivity concentration observed at 30 μg/mL across all assays. However, non-optimal concentrations resulted in markedly divergent responses. 10–20 μg/mL CK failed to upregulate CAT expression, with maximum induction achieved only at 30 μg/mL and partial retention of activity at 40 μg/mL (Figure 5C). In contrast, GSH-Px activity was significantly enhanced by 10–20 μg/mL CK but was not activated at the 40 μg/mL concentration (Figure 5D). As a reference, 0.05% vitamin E showed no significant activation of either CAT or SOD in our assay systems (Figure 5C,E). Additionally, CK significantly enhanced the synthesis of collagen I, III, as well as elastin in HSF cells, while concurrently inhibiting MMP-1 secretion (Figure 6). These findings are consistent with previous reports on the MMP-1-inhibition capacity of CK (Lee et al. 2014). The regulations of ECM homeostasis suggest CK's unique advantage over single-target anti-aging agents such as retinol or vitamin E. Nevertheless, the narrow effective concentration window for elastin synthesis (peak activity at 30 μg/mL) warrants further investigation, potentially reflecting complex feedback regulatory mechanisms or cellular stress thresholds (Figure 6C).

Importantly, the high-density fermentation process for the recombinant β-glycosidase and the downstream biocatalytic synthesis of CK are currently undergoing commercial-scale pilot testing (data not shown), demonstrating exceptional industrialization potential. Scale-up to full commercial production is anticipated in the near future. While the cell-level experimental results presented herein strongly support the superior bioactivity of CK as a cosmetic ingredient, further clinical skin testing is essential and is currently in progress. Comprehensive and systematic investigations into the cosmetic applications of CK, beyond production optimization, are also actively underway to fully realize its market potential as a leading anti-aging cosmetic ingredient.

5 | Conclusions

In summary, this study establishes a robust, scalable, and efficient platform for CK production *via* recombinant β-glycosidase-catalyzed bioconversion, overcoming previous limitations in enzyme availability and catalytic efficiency. The engineered *E. coli* strain achieved high enzyme yields, facilitating a rapid conversion rate of Rb1 to CK with industrial feasibility. Furthermore, CK exhibited exceptional cytocompatibility and multi-target anti-aging effects, including the suppression of ROS, enhancement of ECM synthesis, and inhibition of MMP-1. These attributes highlight CK′s potential as a novel active ingredient in anti-aging cosmetics, providing a natural and sustainable alternative to synthetic compounds. This work not only advances the biomanufacturing of rare ginsenosides but also lays a scientific foundation for the

development of next-generation skincare products focused on holistic skin health. Future efforts should prioritize translational studies to bridge the gap between laboratory-scale production and commercial deployment.

Acknowledgments

The authors have nothing to report.

Conflicts of Interest

The authors declare no conflicts of interest.

Data Availability Statement

The raw data cannot be shared publicly as they contain confidential commercial information. Interested researchers may contact the corresponding author for data access negotiations. The data that support the findings of this study are available from the corresponding author upon reasonable request.

References

Chae, S., K. A. Kang, W. Y. Chang, et al. 2009. "Effect of Compound K, a Metabolite of Ginseng Saponin, Combined With γ-Ray Radiation in Human Lung Cancer Cells In Vitro and In Vivo." *Journal of Agricultural and Food Chemistry* 57: 5777–5782. https://doi.org/10.1021/jf900331g.

Chen, J., M. Si, Y. Wang, et al. 2019. "Ginsenoside Metabolite Compound K Exerts Anti-Inflammatory and Analgesic Effects via Down-regulating COX2." *Inflammopharmacology* 27: 157–166. https://doi.org/10.1007/s10787-018-0504-y.

Dong, L., X. Bian, and Y. Zhao, et al. 2022. "Rhizosphere Analysis of Field-Grown Panax Ginseng With Different Degrees of Red Skin Provides the Basis for Preventing Red Skin Syndrome." *BMC Microbiology* 22: 12. https://doi.org/10.1186/s12866-021-02430-9.

Fu, Y. 2019. "Biotransformation of Ginsenoside Rb1 to Gyp-XVII and Minor Ginsenoside Rg3 by Endophytic Bacteriumflavobacteriumsp. GE 32 Isolated Frompanax Ginseng." *Letters in Applied Microbiology* 68: 134–141. https://doi.org/10.1111/lam.13090.

Kim, K. A., I. H. Jung, S. H. Park, Y. T. Ahn, C. S. Huh, and D. H. Kim. 2013. "Comparative Analysis of the Gut Microbiota in People With Different Levels of Ginsenoside Rb1 Degradation to Compound K." *PLoS One* 8: e62409. https://doi.org/10.1371/journal.pone.0062409.

Koh, E., O. H. Jang, K. H. Hwang, Y. N. An, and B. Moon. 2015. "Effects of Steaming and Air-Drying on Ginsenoside Composition of Korean Ginseng (Panax ginsengc.A. Meyer): Processing Effect on the Ginsenosides of Ginseng." *Journal of Food Processing and Preservation* 39: 207–213. https://doi.org/10.1111/jfpp.12412.

Lee, C. S., I. H. Bae, J. Han, et al. 2014. "Compound K Inhibits MMP-1 Expression Through Suppression of C-Src-Dependent ERK Activation in TNF-α-Stimulated Dermal Fibroblast." *Experimental Dermatology* 23: 819–824. https://doi.org/10.1111/exd.12536.

Lee, J. O., E. Choi, K. K. Shin, et al. 2019. "Compound K, a Ginsenoside Metabolite, Plays an Antiinflammatory Role in Macrophages by Targeting the AKT1-mediated Signaling Pathway." *Journal of Ginseng Research* 43: 154–160. https://doi.org/10.1016/j.jgr.2018.10.003.

Li, C., Y. Dong, L. Wang, et al. 2019. "Ginsenoside Metabolite Compound K Induces Apoptosis and Autophagy in Non-Small Cell Lung Cancer Cells via AMPK–mTOR and JNK Pathways." *Biochemistry and Cell Biology* 97: 406–414. https://doi.org/10.1139/bcb-2018-0226.

Li, C. C., Y. Q. Liu, Y. Wang, H. S. Yu, and F. X. Jin. 2009. "Extraction of Ginsenoside Compound-K." *Journal of Dalian Polytechnic University* 28: 87–89.

Mancuso, C., and R. Santangelo. 2017. "Panax ginseng and Panax quinquefolius: From Pharmacology to Toxicology." *Food and Chemical Toxicology* 107: 362–372. https://doi.org/10.1016/j.fct.2017.07.019.

Noh, K. H., J. W. Son, H. J. Kim, and D. K. Oh. 2009. "Ginsenoside Compound K Production From Ginseng Root Extract by a Thermostable β-Glycosidase From Sulfolobus Solfataricus." *Bioscience, Biotechnology, and Biochemistry* 73: 316–321. https://doi.org/10.1271/bbb.80525.

Pan, W., B. Xue, C. Yang, et al. 2018. "Biopharmaceutical Characters and Bioavailability Improving Strategies of Ginsenosides." *Fitoterapia* 129: 272–282. https://doi.org/10.1016/j.fitote.2018.06.001.

Papaccio, F., A. D'Arino, S. Caputo, and B. Bellei. 2022. "Focus on the Contribution of Oxidative Stress in Skin Aging." *Antioxidants* 11: 1121. https://doi.org/10.3390/antiox11061121.

Park, S. Y., E. A. Bae, J. H. Sung, S. K. Lee, and D. H. Kim. 2001. "Purification and Characterization of Ginsenoside Rb1-Metabolizing β-Glucosidase From Fusobacterium K-60, a Human Intestinal Anaerobic Bacterium." *Bioscience, Biotechnology, and Biochemistry* 65: 1163–1169. https://doi.org/10.1271/bbb.65.1163.

Qin, Y., X. W. Zhou, W. Zhou, X. W. Li, M. Q. Feng, and P. Zhou. 2008. "Purification and Properties of a Novel β-Glucosidase, Hydrolyzing Ginsenoside Rbl to CK, From *Paecilomyces bainier*." *Journal of Microbiology and Biotechnology* 18: 1081–1089.

Shin, Y. W., E. A. Bae, S. S. Kim, Y. C. Lee, and D. H. Kim. 2005. "Effect of Ginsenoside Rb1 and Compound K in Chronic Oxazolone-Induced Mouse Dermatitis." *International Immunopharmacology* 5: 1183–1191. https://doi.org/10.1016/j.intimp.2005.02.016.

Son, J. W., H. J. Kim, and D. K. Oh. 2008. "Ginsenoside Rd Production From the Major Ginsenoside Rb1 by β-glucosidase From Thermus caldophilus." *Biotechnology Letters* 30: 713–716. https://doi.org/10.1007/s10529-007-9590-4.

Wang, S., F. Li, X. Feng, et al. 2025. "Promoting Collagen Synthesis: A Viable Strategy to Combat Skin Ageing." *Journal of Enzyme Inhibition and Medicinal Chemistry* 40: 2488821. https://doi.org/10.1080/14756366.2025.2488821.

Yin, Q., H. Chen, R. H. Ma, et al. 2021. "Ginsenoside CK Induces Apoptosis of Human Cervical Cancer HeLa Cells by Regulating Autophagy and Endoplasmic Reticulum Stress." *Food & Function* 12: 5301–5316. https://doi.org/10.1039/d1fo00348h.

Yoon, S. H., E. J. Han, J. H. Sung, and S. H. Chung. 2007. "Anti-Diabetic Effects of Compound K Versus Metformin Versus Compound K-Metformin Combination Therapy in Diabetic db/db Mice." *Biological & Pharmaceutical Bulletin* 30: 2196–2200. https://doi.org/10.1248/bpb.30.2196.

Yun, T. K. 2001. "Brief Introduction of Panax ginseng C.A. Meyer." *Journal of Korean Medical Science* 16: S3–S5. https://doi.org/10.3346/jkms.2001.16.S.S3.